Indian Journal of Chemical Technology
Vol. 31, March 2024, pp. 248-256
DOI: 10.56042/ijct.v31i2.2547

Structure property relations in chitosan based nanocomposite films using WAXS techniques

Manisha[1], Jagadish R. S[1]*, Roli Verma[1], P. Parameshwara[2] & Baldev Raj[3]
[1]Department of Chemistry, JSS Academy of Technical Education, Noida 201301, Uttar Pradesh, India
[2]Department of Physics, The National Institute of Engineering, Mysore, Karnataka, India
[3]Department of Food Packaging Technology Department, CSIR-CFTRI, Mysore, Karnataka, India
*E-mail: jagadishrs@jssaten.ac.in

Received 10 June 2023; accepted 5 February 2024

In this research, nanocomposite (NC) films comprising chitosan with 20% weight glycerol have been reinforced using three different types of nanoparticles—TiO_2, Ag, and Fe_2O_3 at concentrations of 1%, 3%, and 5% by weight, respectively, in various combinations. The characteristics of these NC films have been compared with those of both pure chitosan and chitosan containing 20% weight glycerol. The incorporation of nanoparticles significantly altered the mechanical and barrier properties of the chitosan films. Notably, the tensile strength have experienced an increase ranging from 22% to 84%, while the water vapour transmission rate (WVTR) decreased by 16% to 56%, depending on the nanoparticle dispersion under consideration. The chitosan 3% Fe_2O_3 NC film have exhibited the lowest WVTR value and the highest tensile strength when compared to the chitosan/3% Ag NC film. The minimum WVTR value has been observed in the chitosan/3% Fe_2O_3 NC film compared to the chitosan film. The materials and their composites have been analyzed using wide-angle x-ray diffraction patterns to calculate microcrystalline characteristics. To explore the microstructural behaviour of the chitosan and TiO_2, Ag, Fe_2O_3 composites and establish a connection with physical characteristics such as tensile strength and percentage elongation, an exponential asymmetric column length distribution function approach has been employed.

Keywords: Antimicrobial properties, Chitosan, Mechanical properties, Nanocomposite film, Nano-TiO_2, Nano-silver, nano-Fe_2O_3

Introduction

The ongoing exploration revolves around harnessing renewable resources to produce packaging materials that are either edible or biodegradable, aiming to enhance product quality and mitigate issues associated with waste disposal. One approach involves utilizing renewable biopolymers derived from plant and animal resources, including proteins, lipids, and their composites[1-6].

Chitosan, a de-N-acetylated form of chitin found in the shells of crabs, shrimp, and other creatures, has garnered significant interest due to its abundance, biocompatibility, biodegradability, non-toxicity, and chemical inertness. Comprising beta (1-4)-2-amino-2-deoxy-D-glucose units with occasional N-acetyl glucosamine residues[6], chitosan stands as the second most common natural polymer. Its attributes make it suitable for creating transparent films, with potential applications in various packaging needs [7, 8]. In addition to its packaging potential, chitosan's antibacterial and metal binding properties have attracted attention from the scientific community[9]. Biopolymer films, incorporating a wide range of additives such as antioxidants, antifungal agents, antibacterial components, colorants, and other nutrients, hold promise for superior packaging materials[10]. Specifically, antimicrobial films based on biopolymers could extend the shelf life of various foods, including meat, fish, poultry, cereals, cheese, fruits, and vegetables[11-13].

However, the use of biopolymers has been limited due to inherent water sensitivity and relatively poor stiffness and strength, especially in humid environments[10]. Researchers have focused on enhancing the physical characteristics of biopolymer films through methods like, mixing, and introducing fillers such as nanoparticles (NPs). Nanocomposite (NC) films/membranes are of particular interest to researchers studying modern materials, as nanotechnology offers a means to enhance material qualities. In this regard, studies have been carried out in Preparation of nanocomposite thin film through interfacial polymerization process of organoclay, Ligninsulfonate/trimesoylchloride nanocomposite membrane with AgNPs,[14-16] m-phenylene diamine and trimesoyl chloride film[17], graphene oxide dots as nano

fillers in separation process[18], cellulose nanofiber mediated natural dye based biodegradable bag[19], cellulose nanocrystal based membrane[20], graphene oxide nanocomposites thin film[21], carbon nanotube thin film nanocomposite[22], Pd-nanoparticles incorporated films [23], nanoclay incorporated films[24], mutiwalled carbon nanotube thin layered film[25], cellulose nanofiber -poly(ethylene terephthalatenano membranes [26].

Various polymers, including polyvinyl chloride (PVC), polyethylene (PE), nylon, and starch, have been investigated as NPs in studies on NC films for food packaging[27-31]. Materials at the nanoscale exhibit a higher surface-to-volume ratio compared to their microscale counterparts, allowing for increased interaction with biological molecules and enhanced efficiency [32]. Moreover, researchers have explored the antibacterial properties of nanostructured materials[33], studying their potential as growth inhibitors[34], killing agents[35-39], and antibiotic transporters[40]. These advancements signify a progressive approach to developing sustainable and effective packaging solutions in the realm of food and materials science.

The existing body of literature reveals a scarcity of research on natural bio-polymer-based nanocomposite (NC) films specifically designed for food packaging[40–41]. Additionally, limited investigations have been identified regarding natural biopolymer nanocomposites and their potential application in antimicrobial films[10, 42–44]. In light of these gaps, the current study aims to address this research void by focusing on the development of biodegradable NC antimicrobial films. Chitosan, along with nano TiO_2, nano Ag, and Fe_2O_3, will be employed with the ultimate goal of creating films possessing desirable qualities suitable for food packaging applications.

Experimental Section

The chitosan powder used in this study was supplied by India Sea Food in Cochin, India, with a batch number of BX 12AN-24. The chitosan had an 88% deacetylation percentage and a viscosity of 195 mPa. To verify the viscosity of the chitosan, Rheology International's RI: 3: M viscometer was utilized in a laboratory setting, maintaining an ambient temperature of 25 ± 2 ℃. Nanoparticles of TiO_2, Ag, and Fe_2O_3, each less than 100 nm in size, were obtained from Sigma Aldrich in St. Louis, Missouri, and were employed in the experimental setup. All other chemicals utilized in the study were procured from S D Fine Chemicals in India and met analytical quality standards.

Preparation of nanocomposite films

2 g of chitosan powder was dissolved in 100 mL of 1% acetic acid solution and 20 wt% glycerol (on the weight basis of the total polymer) while being continuously stirred for 20 min at 90 °C to create chitosan films. To get rid of insoluble contaminants, a homogenous, viscous solution was created and then filtered using cheese cloth. 200 mL of the solution were filtered through cotton and then put onto a separate glass plate measuring 27 cm x 20 cm that was covered in a polyethylene film. After allowing the solution to gradually dry out at room temperature for 3 to 4 days, a translucent film with a consistent thickness was produced. The films were removed after drying and stored at room temperature (25 °C, 50% RH). Additionally, using the solvent intercalation method, chitosan-based NC films were created by combining three different NP types in varying amounts, including 1, 3, and 5 wt% of TiO_2, Ag, and Fe_2O_3.

Each type of nanoparticle (w/w, relative to chitosan on a dry weight basis) was dispersed in a 200 mL 1% acetic acid solution by vigorous mixing for an hour using a magnetic stirrer. Next, NP solution was obtained by sonicating the mixture for 30 min at 60°C with an amplitude of 30% and 0.5 pulses using a probe type ultrasonic processor (VC 750 model, Sonics and Materials Inc., Following the addition of 20% glycerol (on the weight basis of the total polymer) and four grammes of chitosan powder, the NP solution was then agitated for 20 min at 90 °C using a hot plate. The solution was then sonicated for an additional 10 min at 60 °C, and then it was dried using the same process as for casting chitosan films[10, 45].

Physico-mechanical properties

After equilibrating at 65% RH at 27 °C, the physical and mechanical characteristics of chitosan NC films, including as their tensile qualities, rip strength, and burst strength, were assessed.

Tensile properties

Using LLOYD's universal testing machine, the tensile strength and elongation at break of NC films were tested in accordance with ASTM D - 882. (LLOYDS-50K London, UK). The test was run with a 50 mm initial grip separation and a 200 mm/min cross head speed. At a temperature of 28 °C, tensile

strength and elongation at break values were tested both in the machine direction and the cross direction. Five measurements were taken for each property, and an average value with a standard deviation was reported.

Water vapour transmission rate

Aluminum dishes were used to measure the water vapour transmission rate (WVTR) of NC films in accordance with ASTM E-96 [46]. A sample with a diameter of 50 cm^2 was sealed on a cup with a very hydroscopic substance, such as anhydrous $CaCl_2$. After being placed on the cup, the specimen was completely sealed, leaving a 50 cm^2 circular surface area for the exposure using hot wax. The wax-sealed cups were given some rest time to get to room temperature. The humidity chamber, which was kept at 38 °C with 90% RH gradient, was filled with the prepared cups after they had been weighed. As a result, weight increased as a result of $CaCl_2$ absorbing moisture that seeped through the coating. The following equation, which uses the linear least square method, was used to determine WVTR after weight gain graphs were plotted against time;

$$WVTR = Slope\ (wt\ gain/day)/Film\ area\ (m^2)$$

Optical properties

After equilibrating the samples at 65% RH at 27 °C, the optical characteristics of chitosan NC films were assessed using a Suga test, Digital Hazemeter (model HGM-2DP Japan). According to the ASTM D-1003-61 technique, the haze behaviour of dust- and grease-free films was observed.

Statistical analysis

Microsoft Excel's "t" test was used to evaluate whether there were any significant differences between the sample means. Differences were considered significant at p 0.05.

XRD analysis

The Rigaku Miniflex II diffractometer was used to record the wide angle X-ray diffraction (WAXS) patterns of chitosan and its composites (TiO_2, Ag, and Fe_2O_3) using Ni-filtered light with a wavelength of 1.5406 (CuK). Composite films were scanned in continuous mode at a speed of 5 degrees per minute in steps of 0.02°. The evaluation of microstructural characteristics was done using the obtained patterns for line profile analysis[11,46]. Fourier method of Warren and Averbach[47], where an analytical expression for the crystallite size distribution is used also referred to as single order method for line profile analysis. Essentially, intensity profile I versus 2θ was converted into I versus sin θ/λ and then used to compute Fourier coefficients which are functions of the size Fourier coefficient and strain Fourier coefficient. An exponential analytical distribution was used to calculate size Fourier coefficient and hence the intensity profile. This simulated intensity profile was compared with the experimental profile. The input parameters were varied to the effect that one has a set of parameters such as crystallite size (<N>) and strain (g in %) which give a good convergence. For the analysis, X-ray diffraction data was used to simulate the intensity profile by varying the necessary parameters using the equations given in the literature [48,49]. Wide angle XRD patterns of chitosan and glycerol-chitosan based films with nanoparticles like TiO_2, Ag and Fe_2O_3 of different concentrations are used for line profile analysis to estimate microstructural parameters like crystallite size (<N>), percentage lattice strain (g) and surface weighted crystallite size (D_s). Three prominent peaks around 6°, 11° and 20° were used for line profile analysis. Taking into account the presence of intrinsic strain in these films when they are formed, we carried out modelling of the X-ray profiles of the reflections observed.

Results and Discussion

Physico-mechanical properties

Chitosan and nanocomposite films based on chitosan were strong, flexible, semitransparent, and self-standing. The chitosan/TiO_2 nano composite film had a pale yellow appearance, while the chitosan/Fe_2O_3 version had a red appearance. The surface hue of the chitosan/Nano-Silver sheet, however, was grey.

Table 1 displays the tensile strength and percentage elongation values for nano composite films made of chitosan and chitosan-based materials. A 45 MPa tensile strength for ordinary chitosan film was observed. 20% glycerol was added to the chitosan, and it was found that the tensile strength was drastically reduced by 45%, dropping to 24.72 MPa. When compared to glycerol-added chitosan films, tensile strength was shown to have grown to 38.91 MPa for 1% TiO_2 and decreased gradually up to 30.31 MPa for 5% TiO_2 by the reinforcement with three distinct types of nanoparticles in varied

proportions to the chitosan and 20% glycerol combination. Similar to how the tensile strength of Silver-based nanofilms rose, they reached a maximum of 45.54 MPa in 3% Ag, which is nearly, if not quite, higher than that of plain chitosan. Additionally, tensile strength increased similarly in nanofilms made of Fe_2O_3 that contained chitosan. Tensile strength increased to 37.31 MPa at 1% Fe_2O_3 and steadily decreased as Fe_2O_3 nanoparticle concentration increased. The maximum values of tensile strength for chitosan-based nano composite films occur at 1% TiO_2, 3% Ag, and 1% Fe_2O_3 incorporation to the chitosan polymer matrix. These films exhibit a tendency to grow and then decline with increasing nano particle content. This was caused by the polymer matrix's polymer matrix's high interfacial adhesion and dispersion of nanoparticles. When subjected to tensile stress, the force was transmitted to nanoparticles through the interphase, where they then served as the receptor for the force, raising the tensile strength. Additionally, it was shown that tensile strength reduced when nanoparticle concentrations in the polymer matrix exceeded 1 wt% (in the cases of TiO_2 and Fe_2O_3) and 3 wt% (in the case of Ag). The degradation of the interphase and nanoparticles was attributed to the greater propensity of nanoparticles to form agglomerates at higher concentrations.

It was observed that the simple chitosan film had a 16.31% elongation. The % elongation increased to 42.27 with the addition of 20% glycerol to the chitosan, resulting in a significant increase in the flexibility of chitosan films. In TiO_2, Ag, and Fe_2O_3 based chitosan nano films, the percentage elongation was shown to have dropped from 39.16 to 20.21, 41.24 to 37.22, and 39.79 to 34.27, respectively, with the addition of three different types of nanoparticles in various amounts. The final film was discovered to have good flexibility and tensile strength, both of which are required for food packing[50-52].

Barrier properties

Table 1 displays the water vapour transmission rate (WVTR) values for chitosan, chitosan 20% glycerol, and chitosan-based nano composite films. Chitosan and chitosan with 20% glycerol were found to have WVTR values of 4410.73 g/m^2/day and 4895.25 g/m^2/day, respectively. The WVTR rises by around 10% with the addition of glycerol. The WVTR was found to have dropped by 25.32% for 1% TiO_2, 41.36% for 3% TiO_2, and 16.26 for 5% TiO_2 when three different nanoparticles were introduced to the chitosan and 20% glycerol combination, respectively. Similarly, the WVTR of nanofilms based on Ag declined by up to 49.13% for 1%Ag and then steadily decreased to 38.71% for 5%Ag. Additionally, chitosan-based nanofilms with Fe_2O_3 incorporation showed a similar decrease in WVTR. Maximum WVTR reduction of 56.07% occurred at 3% Fe_2O_3. Depending on the nanoparticles utilized, the WVTR of chitosan-based nanocomposite films considerably lowered by 16–56%. It is thought that the existence of ordered dispersed nanoparticle layers with large aspect ratios in the polymer matrix is what causes the decrease in WVTR of chitosan-based nano composite films. This lengthens the effective path length for diffusion by forcing water vapour moving through the film to take a roundabout route through the polymer matrix surrounding the nanoparticles. The emergence of a polymeric composite structure containing nanoparticles may also be to blame for the observed

Table 1 — Physico-mechanical, barrierand optical properties of chitosan and chitosan based nano composites

Materials Films	Tensile strength (MPa)	% Elongation	WVTR (g/m^2/days) at 90% RH gradient at 38 °C	Haze
Plain chitosan (C)	45±0.79	16.31±0.92	4410.73±20.12	11.0
Chitosan + Glycerol(CG)	24.74±0.87	42.27±1.04	4895.25±16.10	9.1
CG+ 1 % TiO_2	38.91±0.72	39.16±0.76	3655.68±27.32	64.9
CG+ 3 % TiO_2	34.23±0.89	22.08±0.96	2870.40±22.06	93.4
CG+ 5 % TiO_2	30.31±0.54	20.21±1.11	4099.20±25.51	94.7
CG+ 1 % Ag	39.05±0.84	41.24±1.41	2489.76±29.08	11.9
CG+ 3 % Ag	45.54±0.43	39.72±0.84	2851.20±28.98	13.1
CG+ 5 % Ag	41.57±0.65	37.22±0.70	3000.00±12.57	17.4
CG+1% Fe_2O_3	37.31±0.95	39.79±0.74	3398.40±23.09	57.0
CG+3% Fe_2O_3	34.69±0.76	38.06±0.66	2150.40±28.79	76.7
CG+5% Fe_2O_3	33.03±0.48	34.27±0.65	3727.68±11.54	89.7

Mean±SD, n=5 for Tensile strength & %elongation, n=3 for WVTR and Haze properties

drop in WVTR. When assessing nano composite films for use in food packaging, protective coatings, and other applications where effective polymer barriers are required, the reduction in WVTR is crucial. This may improve the potential for such films to be used as breathing films in the packing of fresh products.

Optical properties

Table 1 displays the haze values of chitosan and chitosan-based nano composite films. The simple chitosan film was found to have a hazy value of 11. It was found that the haze value dropped to 9.1 after 20% glycerol was added to chitosan. In comparison to chitosan films with glycerol added, haze values increased for TiO_2, Ag, and Fe_2O_3-based chitosan nanofilms from 64.9 to 94.7, 11.9 to 17.4, and 57 to 89.7, respectively, by the integration of three different types of nanoparticles in varying quantities. The rise in haze following the addition of nanoparticles to the chitosan polymer matrix with additional glycerol could be caused by scattering or diffusion of light radiation by nanoparticles.

XRD analysis

Figs 1, 2 and 3 depict the XRD patterns of glycerol-based chitosan films with nanoparticles like TiO_2, Ag, and Fe_2O_3 and glycerol-chitosan-based nano-composites films with TiO_2, Ag, and Fe_2O_3 of various concentrations. To calculate microstructural characteristics such crystallite size and lattice disorder, line profile analysis of all patterns has been done using an exponential distribution function. Table 2 provides the values of the microstructural parameters for all the notable XRD Bragg reflections. Lattice disorder varies between 0.1% and 0.3%.

As a result of the large number of experimentally established factors, including microstructural parameters, tensile strength, elongation, and haze, we have employed multivariate analysis to compare and analyse nanocomposite films quantitatively. Each of these parameters is given weightage "w" in this approach, and the relevant criterion index has been obtained. The microstructural parameters in XRD analysis are calculated for different Bragg angles, and we have created a sub-sectional index P that is provided by

$$P = \frac{\sum w_i D_s(2\theta)}{\sum w_i}$$

Here w_i's are the weightage attributed to individual Bragg's reflections and their value is decided on the basis of their significant presence in the XRD pattern.

We have defined the overall criterion index Q for individual samples and given by

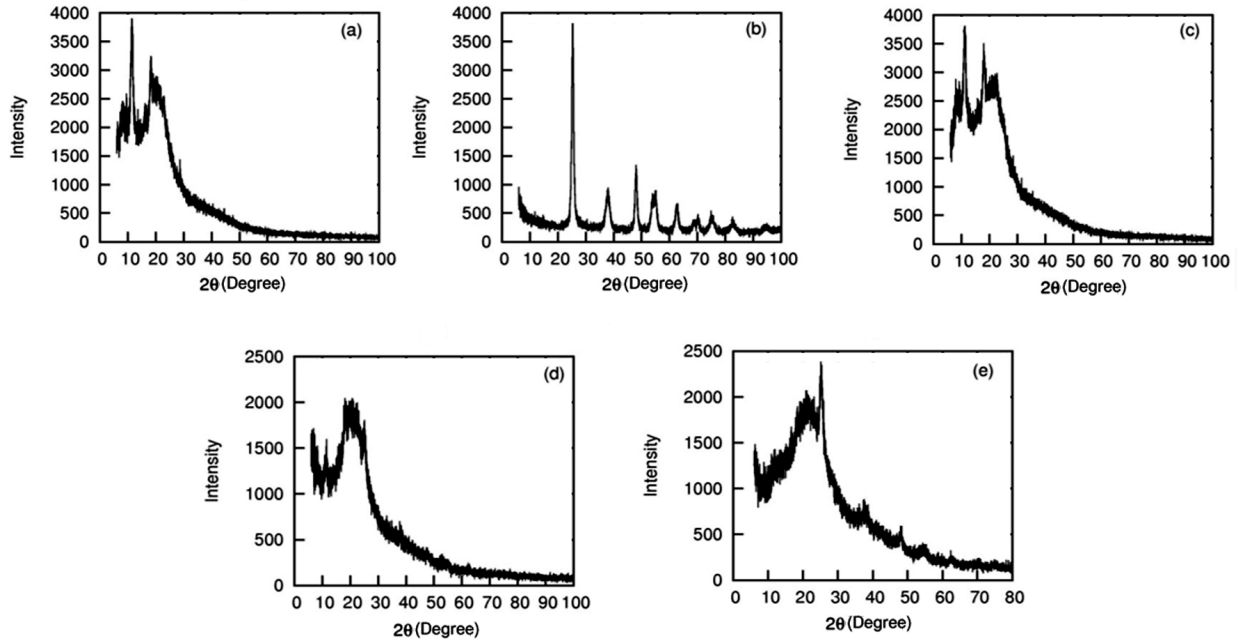

Fig. 1 — X-ray diffraction patterns for chitosan based TiO_2nano composite films: (a) Chitosan with glycerol (CG), b) Pure TiO_2(c) CG +1% TiO_2 (d) CG +3% TiO_2 and (e) CG+5% TiO_2

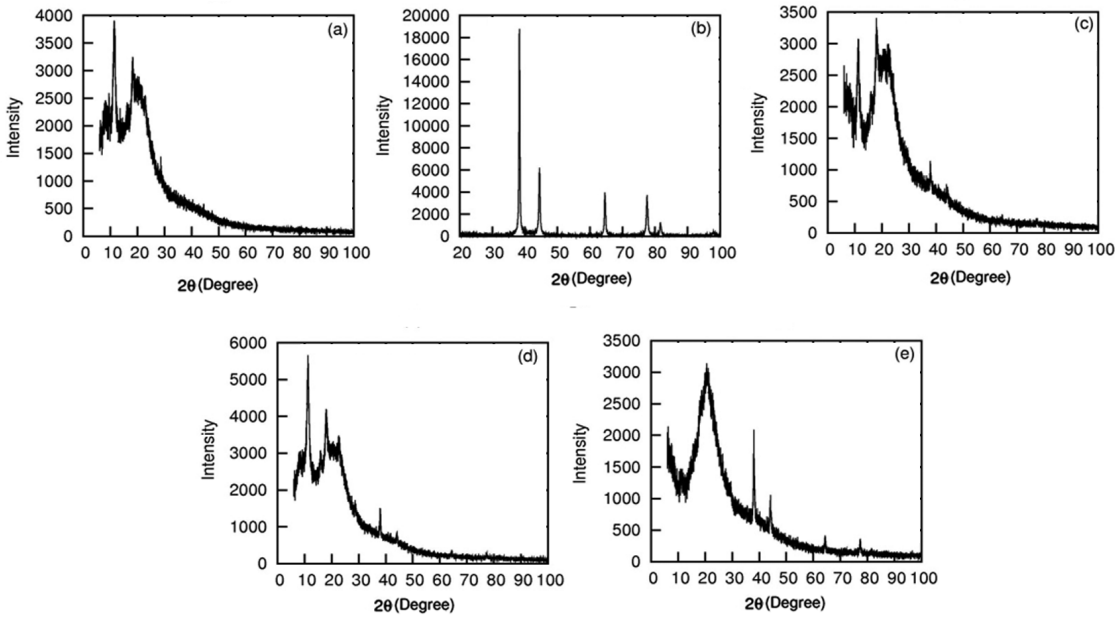

Fig. 2 — X-ray diffraction patterns for chitosan based Ag nanocomposite films: (a) Chitosan with glycerol (CG), b) Pure Ag, (c) CG +1% Ag, (d) CG +3% Ag and (e) CG+5% Ag

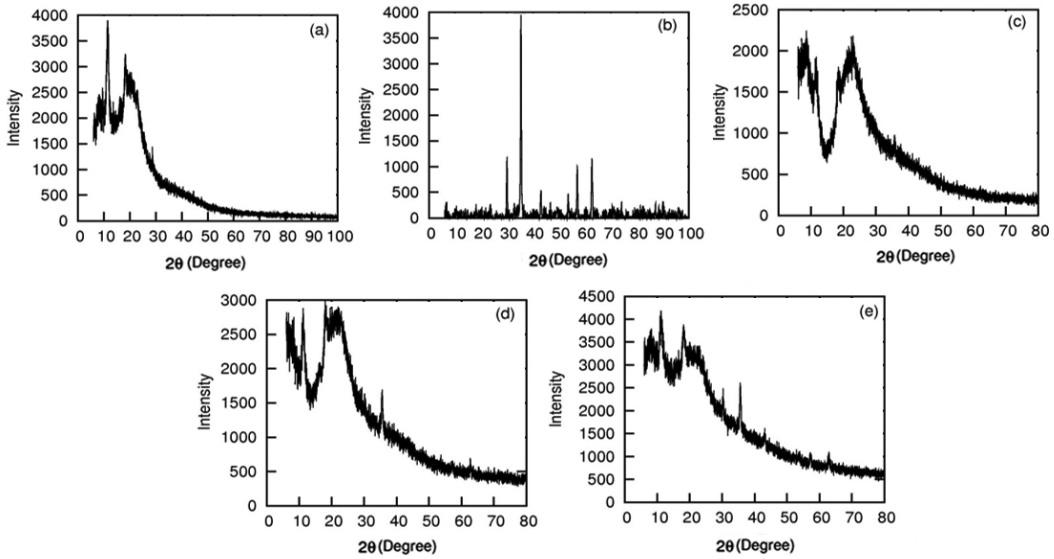

Fig. 3 — X-ray diffraction patterns for chitosan based Fe_2O_3 nanocomposite films: (a) Chitosan with glycerol (CG), (b) Pure Fe_2O_3, (c) CG +1% Fe_2O_3, (d) CG +3% Fe_2O_3 and (e) CG+5% Fe_2O_3

$$Q = \frac{w_1(P) + w_2(TS) + w_3(E) + w_4(Haze)}{w_1 + w_2 + w_3 + w_4}$$

Where, w_1 and w_2 are assigned weights depending on the sample. Table 2 provides the P and Q values for each sample. Q is now a single index that was determined by taking into accounts all of the measured and computed quantities.

As can be shown from Table 3, nearly all nanocomposite films have higher Q indices than the Glycerol-Chitosan film alone. Particularly, the Q values of 1% TiO_2 (39.68), 3% Ag (37.12), 5% Ag (37.47), and 3% Fe_2O_3 (49.78) show that all the physical attributes are evenly distributed across the films. These studies suggest that nanoparticle-based chitosan composite films with 1% TiO_2, 3% Ag, 5%

Table 2 — Microstructural parameters of chitosan based nanocomposite films

Sample	2θ	d (Å)	<N>	g (%)	Ds=<N> d (Å)
Chitosan+Glycerol	11.45	7.72	6.95	0.1	53.65
	20.14	4.41	1.95	0.1	8.59
TiO_2 (Pure)	25.34	3.50	25.47	0.1	89.14
	37.94	2.37	24.55	0.2	58.18
	48.06	1.89	25.07	0.2	47.38
	55.06	1.67	15.01	0.1	25.06
	62.64	1.48	20.10	0.3	29.74
Ag (Pure)	38.30	2.35	49.20	0.1	115.62
	44.47	2.03	53.06	0.2	107.71
	64.60	1.44	50.02	0.1	72.02
	77.54	1.23	41.03	0.1	50.46
Fe (Pure)	30.02	2.97	13.83	0.2	41.07
	35.38	2.53	22.05	0.1	55.78
	57.10	1.61	29.85	0.3	48.05
	62.66	1.48	34.69	0.1	51.34
Chitosan + 1% TiO_2	11.19	7.90	6.84	0.3	54.03
	18.05	4.91	8.41	0.2	41.29
	21.43	4.14	2.16	0.2	8.94
Chitosan + 3% TiO_2	06.34	13.09	1.12	0.1	14.66
	11.41	7.75	3.26	0.2	25.26
	20.96	4.23	2.13	0.1	9.00
Chitosan + 5% TiO_2	21.78	4.07	2.19	0.1	8.91
	25.21	3.53	15.16	0.2	53.51
Chitosan +1% Ag	11.29	7.83	6.95	0.1	54.41
	20.77	4.27	1.76	0.2	7.51
Chitosan+3% Ag	11.25	7.86	7.80	0.1	61.30
	19.92	4.45	1.56	0.3	6.94
Chitosan+5% Ag	20.66	4.29	2.53	0.1	10.85
	38.05	2.36	35.20	0.2	83.07
Chitosan+1% Fe_2O_3	08.26	10.68	1.33	0.3	14.20
	22.48	3.95	2.44	0.1	9.63
Chitosan+ 3% Fe_2O_3	11.24	7.86	15.76	0.2	123.87
	21.94	4.05	2.81	0.2	11.38
Chitosan + 5% Fe_2O_3	11.22	7.88	7.39	0.1	58.23
	18.23	4.86	10.43	0.3	50.68
	21.76	4.08	2.47	0.1	10.07
	25.60	2.52	80.20	0.1	202.10

Ag, and 3% Fe_2O_3 (especially with high Q index values) have well tensile and flexible (% elongation) properties that are very noteworthy and crucial.

Conclusion

Through the intercalation of nanoparticles in the chitosan matrix, the physical, mechanical, and barrier properties of chitosan films were influenced. Depending on the nanoparticle material examined, tensile strength rose by 22–84% while the water vapour transfer rate dropped by 16–56%. Maximum tensile strength of 84% was found in 3% Ag-incorporated chitosan nanofilms, which represents a significant improvement in strength properties. Water barrier properties have also significantly improved, with the maximum extent of WVTR (56%) decreasing in 3% Fe_2O_3-incorporated nanofilms when compared to chitosan glycerol-based films. Further X-ray experiments reveal that nanoparticle-based chitosan composite films made of 1% TiO_2, 3% Ag, 5% Ag, and 3% Fe_2O_3 (particularly with high Q index values) exhibit good tensile and flexible (% elongation) capabilities that are very notable. These modified chitosan based nano films are biodegradable films with suitable qualities for fresh products (greens) and food packaging applications.

Table 3 — Sub-sectional index (P) and overall criterion index (Q) values of microstructural parameters of chitosan based nanocomposite films

Materials films	P	Q
Chitosan + Glycerol(CG)	31.12	30.35
CG+ 1 % TiO_2	32.57	39.68
CG+ 3 % TiO_2	16.80	31.27
CG+ 5 % TiO_2	17.83	29.97
CG+ 1 % Ag	30.96	34.56
CG+ 3 % Ag	34.12	37.12
CG+ 5 % Ag	39.98	37.47
CG+1% Fe_2O_3	11.91	32.40
CG+3% Fe_2O_3	67.62	49.78
CG+5% Fe_2O_3	52.60	44.94

Acknowledgement

The authors wish to thank Principal, JSS Academy of Technical education, Noida and Director, Scientists of CFTRI, Mysore, India, for the opportunity and encouragement for the investigation

References

1 Debeaufort F & Quezada-Gallo J A, Voilley, Edible Films and Coatings: Tomorrow's Packaging: A Review, *Crit Rev Food Sci Nut*, 38 (1998) 299.

2 Krochta J M & De Mulder C J, Edible and biodegradable polymer films: challenges and opportunities, *Food Technol*, 5 (1997) 61.

3 Tharanathan R N, Biodegradable films and composite coatings: past, present and future, *Trend Food Sci Technol*, 14 (2003) 71.

4 Yangbao M, Xiaojie Z, Yuehong Z, Xiaobo L, Xiaohui C, Lin S, Shanshan L & Yanhua Z, Castor oil-based adhesives: A comprehensive review, *Ind Crops Prod*, 209 (2024) 117986.

5 Bhuyan C, Konwar A, Bora P, Rajguru P & Hazarika S, Cellulose nanofiber-poly(ethylene terephthalate) nanocomposite membrane from waste materials for treatment of petroleum industry wastewater, *J Hazard Mater*, 442 (2023) 129955.

6 Srinivasa P C & Tharanathan R N, Chitin/Chitosan-safe, ecofriendly packaging materials with multiple potential uses, *Food Rev Int*, 23 (2007) 53.

7 Kumar R M N V, Muzzarelli R A A, Muzzarelli C, Sashiwa H & Domb A, Chitosan chemistry and pharmaceutical perspectives, *J Chem Rev*, 104 (2004) 6017.

8 Kumar R M N V, A review of chitin and chitosan applications, *React Funct Polym*, 46 (2000) 1.

9 Dutta P K, Tripathi S, Mehrotra G K & Dutta J, Perspectives for chitosan based antimicrobial films in food applications, *J Food Chem*, 114 (2009) 1173.

10 Rhim J W, Hong S I, Park H M & Perry K W N, Preparation and characterization of chitosan-based nanocomposite films with antimicrobial activity, *J Agric Food Chem*, 54 (2006) 5814.

11 Jagadish R S, Raj B, Parameswara P & Somashekar R, Effect of glycerol on structure-property relations in chitosan/poly (ethylene oxide) blended films investigated using wide-angle X-ray diffraction, *Polym Int*, 59 (2010) 931.

12 Labuza T P & Breene W M, Applications of "active packaging" for improvement of shelf-life and nutritional quality of fresh and extended shelf-life foods, *J Food Process Preserv*, 13(1989) 1.

13 Cagri A, Ustunol Z & Ryser E T, Antimicrobial edible films and coatings, *J Food Prot*, 67 (2004) 833.

14 Borah A, Gogoi M, Goswami R, Sarmah H, Hazarika K K & Hazarika S, Thin film nanocomposite membrane incorporated with clay-ionic liquid framework for enhancing rejection of epigallocatechingallate in aqueous media *J Environ Chem Eng*, 10 (2022) 107423.

15 Chao W, Jiajia Z, Xipeng S & Chunhua Z, Ligninsulfonate/ trimesoylchloride nanocomposite membrane with transmembrane nanochannels via bionic cell membrane for molecular separation panel, *J Membr Sci*, 638 (2021) 119692.

16 Borah A, Borah A R, Gogoi M, Goswami R & Hazarika S, Organic exfoliation of hydrophilic bentonite using aliquat 336 and isobutyl(trimethoxy)silane to enhance its activity toward pH-dependent adsorption of Epigallocatechin Gallate, *Clays Clay Miner*, 71 (2023) 430.

17 Jana G, Fatma Y, Petra C, Michal K, Baturalp Y, Martin K, Jan J, Ivan S, Jason E B, Bart V B & Pavel I J, Separation of racemic compound by nanofibrous composite membranes with chiral selector, *J Membr Sci*, 596 (2020) 117728.

18 Goswami R, Gogoi M, Borah A, Sarmah H, Borah A R, Feng X & Hazarika S, Quantum dot- β-Cyclodextrinnanofiller decorated thin film nanocomposite membrane for removal of cationic andanionic dyes from aqueous solution, *Mater Today Chem*, 35 (2024) 101871.

19 Hazarika K K, Konwar A, Borah A, Saikia A, Barman P & Hazarika S, Cellulose nanofiber mediated natural dye based biodegradable bag with freshness indicator for packaging of meat and fish, *Carbohydr Polym*, 300 (2013) 120241.

20 Bora P, Bhuyan C, Rajguruab P & Hazarika S, A Gemini basic ionic liquid and functionalized cellulose nanocrystal-based mixed matrix membrane for CO_2/N_2 separation, *Chem Commun*, 59 (2023) 11320.

21 Gogoi M, Goswami, R, Borah A & Hazarika S, In situ assembly of functionalized single walled carbon nanotube with partially reduced graphene oxide nanocomposite membrane for chiral separation of β, *Sep Purif Technol*, 283 (2022) 120201.

22 Gogoia M, Goswamia R, Ingolea P G & Hazarikaa S, Selective permeation of L-tyrosine through functionalized single-walled carbon nanotube thin film nanocomposite, *Membr Sep Purif Technol*, 233 (2020) 116061.

23 Goswami R, Gogoi M, Borah H J & Ingole P G, Biogenic synthesized Pd-nanoparticle incorporated antifouling polymeric membrane for removal of crystal violet dye, *J Environ Chem Eng*, 6 (2018) 6139.

24 Borah A, Gogoi M, Goswami R, Sarmah H, Hazarika K K & Hazarika S, Thin film nanocomposite membrane incorporated with clay-ionic liquid framework for enhancing rejection of epigallocatechin gallate in aqueous media, *J Environ Chem Eng*, 10 (2022) 107423.

25 Gogoi M, Goswami R, Borah A, Bhuyan C, Samah H & Hazarika S, Functionalized multi-walled carbon nanotube thin-layered hollow fiber membrane for enantioselective permeation of racemic β-substituted-α-amino acids, *J Chem Sci*, 134 (2022) 89.

26 Bhuyan C, Konwar A, Bora P, Rajguru P & Hazarika S, Cellulose nanofiber-poly(ethylene terephthalate) nano-composite membrane from waste materials for treatment of petroleum industry wastewater, *J Hazard Mater* https://www.sciencedirect.com/journal/journal-of-hazardous-materials/vol/442/suppl/C, 442 (2023) 129955.

27 Zou H, Wu S & Shen J, Polymer/Silica nanocomposites: Preparation, characterization, properties, and applications, *Chem Rev*, 108 (2008) 3957.

28 Fischer S, Vlieger J, Batenburg L, Fischer H & Kock T, Green" nano-composite materials-new possibilities for bioplastics, *J Mater*, 16 (2000) 3.

29 Lagaly G, Interaction of alkylamines with different types of layered compounds, *Appl Clay Sci*, 15 (1999) 1.

30 Alexandre M & Dubois P, Polymer-layered silicate nanocomposites: Preparation, properties and uses of a new class of materials, *Mater Sci Eng*, 28 (2000) 1.

31 Giannelis E P, Polymer layered silicate nanocomposites, *Adv Mater*, 168 (1996) 29.

32 Rhim J W & Perry K W, Ng, Natural biopolymer-based nanocomposite films for packaging applications, *Crit Rev Food Sci Nut*, 47 (2007 411.

33 Luo P G & Stutzenberger F J, Nanotechnology in the detection and control of microorganisms, *Adv Appl Microbiol*, 63 (2008) 145.

34 Cioffi N, Torsi L, Ditaranto N, Tantillo G, Ghibelli L & Sabbatini L, Copper nanoparticle/polymer composites with antifungal and bacteriostatic properties, *Chem Mater*, 17 (2005) 5255.

35 Huang L, Li D Q, Lin Y J, Wei M, Evans D & Duan X, Controllable preparation of Nano-MgO and investigation of its bactericidal properties, *J Inorg Biochem*, 99 (2005) 986.

36 Kumar R & Münstedt H, Silver ion release from antimicrobial polyamide/silver composites, *Biomaterials*, 26 (2005) 2081.

37 Lin Y J, Li D Q, Wang G, Huang L & Duan X, Preparation and bactericidal property of MgO nanoparticles on γ-Al_2O_3, *J Mater Sci Mater Med*, 16 (2005) 53.

38 Qi L F, Xu Z R, Jiang X, Hu C & Zou X, Preparation and antibacterial activity of chitosan nanoparticles, *Carbohydr Res*, 339 (2004) 2693.

39 Stoimenov P, Klinger R L, Marchin G L & Klabunde K J, Metal oxide nanoparticles as bactericidal agents, *Langmuir*, 18 (2002) 6679.

40 Gu H W, Ho P L, Tong E, Wang L & Xu B, Presenting Vancomycin on nanoparticles to enhance antimicrobial activities, *Nano Lett*, 3 (2003)1261.

41 Chawengkijwanich C & Hayata Y, Development of TiO_2 powder-coated food packaging film and its ability to inactivate *Escherichia coli* in vitro and in actual tests, *Int J Food Microbiol*, 123 (2008) 288.
42 Gelover S, Gómez L A, Reyes K & Leal M T, A practical demonstration of water disinfection using TiO_2 films and sunlight, *Water Res*, 40 (2006) 3274.
43 Rabea E I, Badawy M E, Stevens C V, Smagghe G & Steurbaut W, Chitosan as antimicrobial agent: applications and mode of action, *Biomacromolecules*, 4 (2003) 1457.
44 Liau S Y, Read D C, Pugh W J, Furr J R & Russell A D, Interaction of silver nitrate with readily identifiable groups: relationship to the antibacterial action of silver ions, *Lett Appl Microbiol*, 25 (1997) 279.
45 Sondi I & Salopek-Sondi B, Silver nanoparticles as antimicrobial agent: a case study on E. coli as a model for Gram-negative bacteria, *J Colloid Interface Sci*, 275 (2004) 177.
46 Jagadish R S, Raj B, Parameswara P & Somashekar R, Structure–property relation in polyvinyl alcohol/starch composites, *J Appl Polym Sci*, 59 (2012) 1.
47 Warren B E & Averbach B L, The effect of cold-work distortion on X-ray patterns, *J Appl Phys*, 21 (1950) 595.
48 Sangappa S, Mahesh S, Somashekara R & Subramanya G, Analysis of diffraction line profile from silk fibers using various distribution functions, *J Polym Res*, 12 (2005) 465.
49 Gubicza, Reliability and interpretation of the microstructural parameters determined by X-ray line profile analysis for nanostructured material, *Europ Phys J Spec Top*, 231 (2022) 4153.
50 Liu J, Chu T, Cheng M, Su Y, Zou G & Hou S, Bovine serum albumin functional grapheme oxide membrane for effective chiral separation, *J Membr Sci*, 668 (2023) 121198.
51 Gogoi M, Goswami R, Borah A, Sarmah H, Rajguru P & Hazarika S, Amide functionalized DWCNT nanocomposite membranes for chiral separation of the racemic DOPA, *Sep Purif Technol*, 279 (2021) 119704.
52 Goswami R, Gogoi M, Borah A, Sarmah H, Ingole P G & Hazarika S, Functionalized activated carbon and carbon nanotube hybrid membrane with enhanced antifouling activity for removal of cationic dyes from aqueous solution, *Environ Nanotechnol Monit Manag*, 16 (2021) 100492.